

A study of three butterflies: entanglement wedge method, OTOC and pole-skipping

Banashree Baishya¹ Adrita Chakraborty^{2,3} Nibedita Padhi⁴

¹*Department of Physics, Indian Institute of Technology Guwahati, North Guwahati-781039, India*

²*Faculty of Physics and Applied Computer Science,*

AGH University of Krakow, al. A. Mickiewicza 30, 30-059 Krakow, Poland

³*Department of Physics, National Tsing-Hua University, Hsinchu 30013, Taiwan*

⁴*Department of Physics, Indian Institute of Technology Kharagpur, Kharagpur, 721302, India*

E-mail: b.banashree@iitg.ac.in, achakraborty@agh.edu.pl,
nibedita.phy@iitkgp.ac.in

ABSTRACT: In this work, we investigate two salient chaotic features, namely Lyapunov exponent and butterfly velocity, in the context of an asymptotically Lifshitz black hole background with an arbitrary critical exponent. These features are computed using three methods: entanglement wedge method, out-of-time-ordered correlator computation and pole-skipping. We present a comparative study of the aforementioned features where all of these methods yield exactly similar results for the butterfly velocity and Lyapunov exponent. This establishes an equivalence between all three methods for probing chaos in the chosen gravity background. Furthermore, we evaluate the chaos at the classical level by computing the eikonal phase and Lyapunov exponent from the bulk gravity. These quantities emerge as nontrivial functions of the anisotropy index. By examining the classical eikonal phase, we uncover different scattering scenarios in the near-horizon and near-boundary regimes. We also discuss potential limitations regarding the choice of the turning point of the null geodesic in our approach.

KEYWORDS: Chaos, Lifshitz holography

Contents

1	Introduction	1
2	Asymptotically Lifshitz black hole	5
3	Analyses of quantum chaos	6
3.1	Entanglement wedge method	6
3.2	Out-of-Time-Ordered correlators	8
3.2.1	Kruskal extension	9
3.2.2	Gravitational backreaction due to shock wave	10
3.3	Pole-skipping	13
4	Analysis of classical chaos	15
4.1	Null geodesic	15
4.2	Eikonal phase shift	16
4.3	Lyapunov exponent	18
5	Conclusion	19

1 Introduction

The presence of chaos is robust in various disordered many-body systems, as evidenced by the study of black holes. Dynamical phenomena such as the growth of local perturbations due to sufficiently small changes in the initial conditions, the resulting deviations in the trajectory, and the scrambling of quantum information, are some immediate consequences of chaos in disordered systems. The Anti-de Sitter (AdS)/Conformal Field Theory (CFT) correspondence, established by [1, 2] provides one of the most competent platforms to realise conformally invariant strongly interacting quantum field theories through their dual AdS background containing the field theory on its boundary. Such holographic duality can also be extended as general gauge/gravity duality where the field theory breaks conformal invariance and its dual geometry is eventually a non-AdS one. A class of nonrelativistic Lifshitz field theories are such theories that follow Lifshitz scaling symmetry

$$t \rightarrow \Omega^\xi t, \quad \vec{x} \rightarrow \Omega \vec{x}, \quad (1.1)$$

characterized by the dynamical critical exponent $\xi \in \mathbb{R}$, $\xi \geq 1$. Such QFTs break Lorentz invariance due to the presence of an anisotropic scale factor along the temporal direction and thus do not adhere to CFT. The holographic dual of Lifshitz field theories is the nonrelativistic Lifshitz geometry which shares similar scale symmetry [3–7]. Exploration of such theories finds its significance in the context of the correlation between high energy

physics and condensed matter physics due to the fact that these theories, especially for $\xi = 2$, are directly related to strongly correlated electron systems. A series of research for rigorous understanding of such field theories have been going on over the last decade by implementing various perspectives [8–12]. One of the crucial features of such theories is the appearance of chaos caused by the dynamic quantum critical point. Previously the holographic Lifshitz bulk spacetime has been found to possess chaotic behaviour of any probe circular string moving in it [13]. In addition to this, the nonintegrability of the class of hyperscale violating Lifshitz theories are studied in [14]. Apart from classical chaos, the chaotic growth of marginally irrelevant operators in 2+1D Lifshitz field theory with $\xi = 2$, also famously known as the quantum Lifshitz model, is previously explored in [15] by using a perturbative approach. Holographic studies on scrambling properties have been done [16] for generic gravitational theories including the asymptotically Lifshitz black hole which reads as the plausible gravity dual of the finite temperature counterpart of Lifshitz field theories[3].

In this article, we aim to study the chaotic properties of such a theory from the bulk perspective. There are many ways to study quantum chaos such as Random matrices [17], Complexity [18–20], Ergodicity [21, 22] etc. But, in this work, we will implement three well-known methods in bulk gravity. In a recent study[23], the butterfly effects of higher derivative gravity theories are analysed by two equivalent holographic understandings, to name, using the method of entanglement wedge reconstruction and incorporating localized gravitational shock waves at the horizon of the corresponding dual black hole. Our agenda in this paper is to check the equivalence of the following three methods of computing quantum chaos for the asymptotically Lifshitz black hole :

- Entanglement wedge method [23–25]
- Out of time-ordered correlation function (OTOC) [15, 26–35]
- Pole-skipping [36–47]

(A) In AdS/CFT correspondence, entanglement wedge reconstruction [48–50] depicts that all the information of the entanglement wedge in the bulk lies in the boundary region. When we perturb the boundary state by a local operator and let the system evolve, then the information gets scrambled in the whole space at a late time. This information propagates outward with a constant velocity. The whole scenario has a bulk description. Perturbing the boundary means probing a particle close to the asymptotic boundary, which is falling toward the black hole in the bulk. This particle then follows a trajectory that reaches inside the extremal surface, also known as the Ryu-Takayanagi(RT) surface [51]. As the trajectory of the particle changes, the RT surface changes its shape. At late time, this RT surface reaches up to the near-horizon region of the black hole with a constant velocity – butterfly velocity (v_B). This method is very well-known for extracting the butterfly velocity [52]. In higher-derivative gravity theories also, this method is well understood [23]. In our work, we employ this method to calculate the butterfly velocity in the Einstein-Proca-type Lifshitz gravity

theory. The action of such theories contains a massive vector field that breaks Lorentz symmetry[53]. It is very motivating to study the chaotic properties of such a theory.

- (B) Quantum chaos can further be studied by calculating the double commutator of any two generic operators V and W as,

$$C(t) = \langle V^\dagger(0)W^\dagger(t)W(t)V(0) + V^\dagger(0)W^\dagger(t)W(t)V(0) - \underbrace{W^\dagger(t)V^\dagger(0)W(t)V(0) - V^\dagger(0)W^\dagger(t)V(0)W(t)}_{\text{out-of time-ordered}} \rangle_\beta. \quad (1.2)$$

The out-of-time-ordered correlators (OTOC) show a large value until the "scrambling time" [54, 55] and decrease rapidly thereafter. The decrease of OTOC leads to an increase of $C(t)$ and signifies the butterfly effect. OTOC has been rigorously studied in connection to black holes and quantum chaos [26–30]. To mention the field theory perspective, OTOC has been computed in 2D CFT [31, 32], Ising chain [33], rational CFT [34], driven CFT [35] and numerically in the quantum Lifshitz model [15]. Study of the commutator in holographic systems [26, 30] generalizes the expression (1.2) to,

$$C(t, x) \approx \exp\left\{\lambda_L \left(t - t_* - \frac{|x|}{v_B}\right)\right\}, \quad (1.3)$$

where the operators are separated by a spatial distance x . The exponent λ_L is called the Lyapunov exponent, v_B is the butterfly velocity and t_* is the scrambling time. The scrambling time is defined as the time at which the commutator square $C(t)$ in (1.2) becomes of order $\mathcal{O}(1)$. In two-derivative gravity, this Lyapunov exponent and butterfly velocity is bounded as [27, 52],

$$\lambda_L \leq \frac{2\pi}{\beta}, \quad v_B \leq v_B^{\text{sch}} = \sqrt{\frac{d}{2(d-1)}}, \quad (1.4)$$

where β is the inverse temperature and v_B^{sch} is the butterfly velocity for a $d+1$ - dimensional AdS-Schwarzschild black brane. A natural question one can ask is whether a theory with broken Lorentz invariance can lead to a violation of this Lyapunov exponent and butterfly velocity bound (1.4). In this paper, we have addressed this question.

- (C) The chaotic nature we discussed in the previous two methods can be captured in the properties of a two-point energy density correlation function at the *pole-skipping* [36–39] point and those points are holographically related to the near-horizon properties of the metric perturbation in bulk. Pole-skipping (P-S) occurs when lines of poles and zeros of retarded Green's function intersect, i.e., a would-be pole gets skipped! At these specific values of the frequency and momentum (P-S point), Green's function is not uniquely defined [56, 57]. These specific values of the frequency (ω_*) and

momentum (k_*) in the energy-density two-point function are connected to the measure of chaos [36, 37] through the following relations:

$$\omega_* = i\lambda_L, \quad k_* = \frac{i\lambda_L}{v_B}, \quad (1.5)$$

where λ_L and v_B are the Lyapunov exponent and the butterfly velocity respectively. In this paper, we have checked whether pole-skipping is a good diagnostic in a theory with broken Lorentz invariance or not. A plethora of studies have so far explored the chaotic nature of the holographic systems utilizing this P-S method in the black hole background [37, 39, 58, 59], plasma physics [41–43], conformal field theories [60–62], holographic system with chiral anomaly [44, 63], with stringy corrections [38], higher derivative corrections [45, 59, 64], brane set-up [46] etc. This phenomenon has been extensively studied in various contexts and explored in different directions in [65–73].

We calculate the butterfly effect in asymptotically Lifshitz black holes using three distinct methods: the entanglement wedge, out-of-time-ordered correlator (OTOC) computation, and pole-skipping. Our analysis compares the results obtained from these methods, demonstrating their equivalence. In [16], the authors determined the scrambling time in Kruskal coordinates for the Lifshitz black hole. However, the explicit forms of the Lyapunov exponent and butterfly velocity for black holes with arbitrary anisotropy have yet to be fully explored in the context of OTOCs. Our primary objective is to calculate these two parameters using all the aforementioned methods, thereby providing a comprehensive understanding of the chaotic properties of Lifshitz black holes.

In addition to the comparative analysis of the quantum chaos, we also elaborate on the eikonal phase in the heavy-heavy-light-light gravitational scattering and the Lyapunov exponent, from the classical perspective. The eikonal phase is priorly known to be related to the deflection angle of the null geodesic of a gravity background [74–76]. It also finds its own significance in the AdS/CFT holography, see [77–79] for review. To compute for eikonal phase shift, the null geodesic equation plays a dominant role in determining the impact parameter, often taken as the ratio of conserved momenta to conserved energy, which eventually affects the nature of the eikonal phase. For real and imaginary eikonal phases, one must obtain elastic and completely nonelastic gravitational scattering respectively. Here in our article, we wish to see how the anisotropy of our chosen gravity background causes different kinds of eikonal phase and thus the results in different scatterings when we shift the extrema of the null geodesic from near boundary to near horizon limit. We verify the eikonal phase using the WKB approximation of the equation of motion of a scalar field. Specifically, we examine for a probable matching of the eikonal phase yielded from both the methods. Furthermore, we wish to briefly exhibit the classical nature of the Lyapunov exponent in the anisotropic background and its consistency with the restrictions that we must impose on the choices of the extrema for the validity of our study.

We organize the paper as follows. In section 2, we give a brief idea of the Lifshitz black hole. In section 3, we perform the explicit calculation of Lyapunov exponent and butterfly velocity using all three methods as explained above. Section 4 is devoted to the

computation of the eikonal phase and Lyapunov exponent via a classical approach. We utilize the notion of geodesic stability to accomplish our purpose here. In section 5, we conclude with an elaborate discussion of the implications of our results for both classical and quantum chaos as well as some future scopes.

2 Asymptotically Lifshitz black hole

In this section, we briefly revisit the black hole geometries that asymptote the nonrelativistic planar Lifshitz background. Such black holes were first developed in [80] for $d = 2$, $\xi = 2$. These black hole solutions are found to consistently satisfy the equations of motion of the Einstein-Proca type gravity theories with the inclusion of a massive vector field [81],

$$\mathcal{S} = \frac{1}{2\kappa^2} \int d^{d+1}x \sqrt{-g} \left[\mathcal{R} - 2\Lambda - \frac{1}{4} F_{\mu\nu} F^{\mu\nu} + \frac{1}{2} m^2 A_\mu A^\mu \right], \quad (2.1)$$

$$F_{\mu\nu} = \partial_\mu A_\nu - \partial_\nu A_\mu.$$

Here, for any $(d+1)$ dimensional Lifshitz black hole, the cosmological constant Λ must be a negative quantity that depends on the anisotropy index ξ as $\Lambda = \frac{d-1}{2(d+1)} \mathcal{R}(\xi)$. Again, $F_{\mu\nu}$ is the electromagnetic field strength. The appearance of a massive vector field with mass m in the above action causes the breaking of the Lorentz invariance in the corresponding metric. The generic form of the $(d+1)$ dimensional Lifshitz black hole solution of the above action can be written as,

$$ds^2 = \frac{R^2}{z^2} \left[-\frac{R^{2(\xi-1)}}{z^{2(\xi-1)}} f(z) dt^2 + d\vec{x}_{d-1}^2 + \frac{dz^2}{f(z)} \right], \quad (2.2)$$

$$f(z) = 1 - \left(\frac{z}{z_h} \right)^{d-1+\xi}.$$

R is the AdS radius, z is the radial coordinate and z_h is the black hole horizon. This geometry asymptotically reaches the planar Lifshitz spacetime

$$ds^2 = \frac{R^2}{z^2} \left[-\frac{R^{2(\xi-1)}}{z^{2(\xi-1)}} dt^2 + d\vec{x}_{d-1}^2 + dz^2 \right]. \quad (2.3)$$

Similarly as the planar Lifshitz spacetime, the Lifshitz black hole geometry also follows anisotropic scaling along the time and space directions

$$t \rightarrow \Omega^\xi t, \quad z \rightarrow \Omega z, \quad \vec{x} \rightarrow \Omega \vec{x}, \quad (2.4)$$

that breaks the Lorentz invariance. Equation (2.2) describes a one-parameter family of linearly charged Lifshitz black holes that are thermodynamically stable and become extremal at the vanishing size [82]. The thermodynamics of such an asymptotically Lifshitz black hole can be reproduced from the holographic renormalization of the gravity theory represented by the action (2.1) [10]. The legitimate dual field theory that lives on the boundary of Lifshitz black hole geometry is the finite temperature version of the non-relativistic Lifshitz

field theories. When we take 2D thermal CFT, the flat boundary that accommodates the CFT is compactified along the time direction and becomes a cylinder. This compactification is done by taking $t \rightarrow t + \beta$, where β gives the circumference of the compactifying circle. Thus β acquires the dimension of length. Now, let us consider a similar compactification of the boundary in the case of thermal LFT for which the dimension of time is $[\text{length}]^\xi$ due to Lifshitz scaling. Thus if we take $t \rightarrow t + \tilde{\beta}$ with the analogy of thermal CFT for the compactification, then $\tilde{\beta}$ should have the dimension of time. Thus we can assume the inverse temperature of thermal LFT as $\tilde{\beta} = \beta^\xi$, where β is the inverse temperature of the thermal CFT. Hence, in the dual bulk side, the temperature of the Lifshitz black hole will also be $T = \frac{1}{\beta^\xi}$. The temperature of the black hole is given by

$$T = \frac{1}{z_h^\xi} \frac{d-1+\xi}{4\pi} = \frac{1}{\beta^\xi} \equiv \frac{1}{\tilde{\beta}}. \quad (2.5)$$

Note that, $\tilde{\beta}$ has dimension of length. For maintaining simplicity in our further calculations, we will denote $\tilde{\beta}$ as β . In the next section, we start with the $(d+1)$ -dimensional Lifshitz black hole geometry given in (2.2) to analyse the chaotic features via a quantum approach.

3 Analyses of quantum chaos

In this section, we will show the explicit calculations of the three methods that we are interested in to study the chaotic parameters. Our focus is to compare these results and see the similar dependence of the chaotic parameters on the anisotropy.

3.1 Entanglement wedge method

As discussed in the introduction, we aim in this subsection to find the butterfly velocity with the entanglement wedge method. For this, we need to calculate the size of the smallest boundary region whose entanglement wedge encloses the infalling particle as shown in Figure 1. In this pictorial description, we can see that $z = 0$ is the boundary and $z = 1$ is the horizon of the black hole. A particle (shown by the red dot) is on the RT surface (shown by the light teal portions) bounded by the boundary region. In general, the RT surface location is determined by extremizing the holographic entanglement entropy functional. We can write the entropy functional as,

$$S_{\text{EE}} = 2\pi \int d^{d-1}y \sqrt{\gamma}, \quad (3.1)$$

where γ is the determinant of the induced metric and y is the set of coordinates on an appropriate codimension-2 surface.

Now, we will use background (2.2) for this wedge method. At a constant t hypersurface ($dt = 0$) and parameterizing z as $z(r)$ with assumption $r = |x^i|$, we can write the induced metric as,

$$\gamma_{\alpha\beta} dx^\alpha dx^\beta = \frac{R^2}{z^2} \left[\left(1 + \frac{z'^2}{f(z)} \right) dr^2 + r^2 d\Omega_{d-2}^2 \right]. \quad (3.2)$$

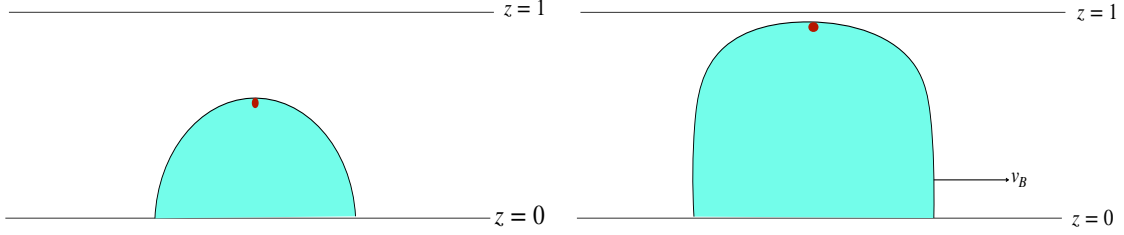


Figure 1. A particle (red dot) is enclosed in the RT surface (light teal)

Note that in the (2.2), the near-horizon limit is achieved by $z = 1$ limit and the boundary limit is achieved by $z = 0$ limit. As we will work with the near-horizon region ($z = 1$), we define the RT surface in the $z = 1$ limit by,

$$z(r) = 1 - \epsilon y(r)^2, \quad (3.3)$$

where we parameterize the near-horizon limit ($z = 1$) with a new function $y(r)$. The coefficient $\epsilon (> 0)$ is a very small number and the function $y(r)$ is the RT profile, which we will solve from the RT equation by performing a Taylor series expansion around $\epsilon = 0$. Now, expanding the induced metric up to order ϵ , we get,

$$\begin{aligned} \gamma_{\alpha\beta} dx^\alpha dx^\beta &= R^2 \left[\left(\frac{4\epsilon^2 y^2 y'^2}{(1-\epsilon y^2)^2 f_1(1-z)} + \frac{1}{(1-\epsilon y^2)^2} \right) dr^2 + \frac{r^2}{(1-\epsilon y^2)^2} d\Omega_{d-2}^2 \right], \\ &= R^2 \left[\left(1 + 2\epsilon \left(y^2 + \frac{2}{f_1} y'^2 \right) \right) dr^2 + r^2 (1 + 2\epsilon y^2) d\Omega_{d-2}^2 + \mathcal{O}(\epsilon^2) \right], \end{aligned} \quad (3.4)$$

where we Taylor expand the factor $f(z)$ near the horizon up to the first order as $f(z) \approx f_1(1-z)$. The determinant of the induced metric is given by,

$$\sqrt{\gamma} = R^2 r^{d-2} \left[1 + \epsilon \left((d-1)y(r)^2 + \frac{2}{f_1} y'(r)^2 \right) \right] + \mathcal{O}(\epsilon^2). \quad (3.5)$$

Now, we can write the RT equation by varying the above equation with respect to $y(r)$. Keeping terms only up to order ϵ , we get,

$$(d-1)y(r) - \frac{2}{f_1} \left(y''(r) + (d-2) \frac{y'(r)}{r} \right) = 0. \quad (3.6)$$

Solving this second-order differential equation, we get,

$$y(r) = r^n [J_n(\mu r) + Y_n(\mu r)], \quad (3.7)$$

where J_n and Y_n are the Bessel functions of first kind and second kind respectively. In the above equation,

$$n = \frac{1}{2}(d-3), \quad \mu = \sqrt{\frac{(d-1)(d-1+\xi)}{2}}. \quad (3.8)$$

Here, the scaling parameter μ is behaving as the momentum. From the eq. (3.3), we can see that near the horizon $z = 1$, the function $y(r)$ takes the form of 0. So, we will see the form of these Bessel functions near $r = 0$. At this vicinity, both these Bessel functions will behave as $\sim \mu^n$. Following [23], where the authors have calculated the butterfly velocity with an exponential ansatz; here in this paper, we have prescribed a more general result for calculating butterfly velocity without taking any ansatz.

The surface enclosing the particle is approaching the horizon at a constant speed, termed as butterfly velocity (v_B). We assume that at each point in time, the tip of the RT surface touches the particle which is visualised by demanding $y(r = 0, t) \sim e^{-\frac{2\pi}{\beta}t}$. Therefore, with the value of μ , we can calculate the butterfly velocity as,

$$v_B = \frac{2\pi}{\beta\mu} = \frac{2\sqrt{2}\pi}{\beta\sqrt{(d-1)(d-1+\xi)}}. \quad (3.9)$$

So, the butterfly velocity v_B becomes (at $z_h = 1$),

$$v_B = \sqrt{\frac{d-1+\xi}{2(d-1)}}. \quad (3.10)$$

This is the butterfly velocity for a $d + 1$ - dimensional Lifshitz black hole. In $\xi \rightarrow 1$ limit, we are getting the planar black hole result $v_B = \sqrt{\frac{d}{2(d-1)}}$. So, the anisotropy affects the butterfly velocity nontrivially. Butterfly velocity characterizes the propagation of chaos in a local system. It has been observed previously that the chaotic feature of the Lifshitz invariant system increases for large ξ values, in other words, for large anisotropy. From the expression of v_B that we get, it is obvious that v_B increases monotonically with ξ for any fixed dimension of the bulk. Thus, the chaotic feature of the asymptotic Lifshitz black hole monotonically increases with larger anisotropy which is consistent from the previous results.

In the next subsection, we will demonstrate the appearance of similar butterfly velocity in the context of out-of-time-ordered correlators.

3.2 Out-of-Time-Ordered correlators

In this subsection, we will study the out-of-time-ordered correlator (OTOC) for thermal Lifshitz field theory dual to a linearly charged asymptotically Lifshitz black hole. It is convenient to study the OTOC in the Kruskal-Szekeres form of the bulk metric, which smoothly covers the globally extended space-time. In Kruskal geometry, the OTOC can be interpreted as the two-particle gravitational scattering between particles moving along the two horizons [27–30]. We shall compute the OTOC in the specific dual-field theory in the form given as

$$\langle \hat{W}(t_2, x_2) \hat{V}(t_1, x_1) \hat{W}(t_2, x_2) \hat{V}(t_1, x_1) \rangle_\beta, \quad (3.11)$$

where we consider $t_2 - t_1 \gg \beta$. The particles that participate in the gravitational scattering process are the operators \hat{W} and \hat{V} , which are inserted in the dual thermofield double (TFD) state. Though the quantity (3.11) is one-sided, our whole computation of the OTOC has been done in a two-sided geometry. So far, the OTOC via the gravitational scattering

process has been explored with various black hole backgrounds [25, 27–30, 39, 40, 83–88]. In our work, we have calculated this quantity (3.38) for a linearly charged asymptotically Lifshitz black hole with arbitrary anisotropy. In the Lifshitz background, the authors of [16] have calculated the scrambling time, though the background they worked with is slightly different from ours. Here, we have provided an explicit calculation of the Lyapunov exponent and butterfly velocity in the two-sided geometry, which yields interesting results.

3.2.1 Kruskal extension

To study the out-of-time-ordered correlators, let us first construct the Kruskal extension of the (2+1) dimensional Lifshitz black hole. We will start with the metric (2.2), but replacing $z = 1/r$ and considering the AdS radius to be 1 for simplicity,

$$ds^2 = -r^{2\xi} f(r) dt^2 + \frac{1}{r^2} \frac{dr^2}{f(r)} + r^2 dx^2, \quad (3.12)$$

and the blackening factor $f(r)$ is given by,

$$f(r) = 1 - \left(\frac{r_h}{r}\right)^{1+\xi}. \quad (3.13)$$

r is the radial coordinate and r_h is the black hole horizon in the emblackening factor $f(r)$. In [89, 90], nonlinearly charged Lifshitz black holes with one and two horizons are obtained with the Eddington-Finkelstein form of the metric. In this case, nonlinearity appears in the blackening factors, and it is characterized by using some extra parameters along with the dynamical exponent ξ of the Lifshitz black hole. Single horizons and double horizons for such black holes are obtained by using specific parametric conditions. However, for the metric in (3.12), we will construct an explicit form of the linearly charged thermal Lifshitz black hole with double horizons by using the Kruskal-Szekeres coordinates. To work in these coordinates, we transform,

$$u = e^{\frac{\alpha}{2}(r_* - t)}, \quad v = e^{\frac{\alpha}{2}(r_* + t)}, \quad (3.14)$$

where α is a function of r_h that relates with the finite temperature T of the black hole as $\alpha \equiv 2\pi T$. The tortoise coordinate r_* will play a very crucial role in defining the smooth horizon in the (u, v) coordinate. We define,

$$r_*(r) = \int \frac{dr}{r^{1+\xi} f(r)} = \int \frac{dr}{r^{1+\xi} \left[1 - \left(\frac{r_h}{r}\right)^{1+\xi}\right]}. \quad (3.15)$$

Integrating equation (3.15), we get,

$$r_*(r) \approx \frac{r^{-\xi}}{\xi(1+\xi)} {}_2F_1\left(1, -\xi, 1-\xi, \frac{r}{r_h}\right). \quad (3.16)$$

We consider $f(r) = (r - r_h)f'(r_h)$ while solving the above equation. Now, taking the near-horizon limit ($r \rightarrow r_h$) of the whole solution, we get,

$$r_* \approx \frac{1}{r_h^\xi(1+\xi)} \log\left(\frac{r - r_h}{r_h}\right). \quad (3.17)$$

As there is a relation between (u, v) coordinate and r_* (from (3.14)), we can easily write,

$$uv = e^{\alpha r_*} \approx \left(\frac{r - r_h}{r_h} \right). \quad (3.18)$$

This equation allows us to claim that the $uv = 0$ is the same limit as the $r = r_h$. This result will be quite helpful for the analysis afterwards. Writing the metric (3.12) in terms of the null coordinates u and v , we get

$$ds^2 = \frac{4r(u, v)^{2\xi}}{\alpha^2 uv} f(r(u, v)) du dv + r(u, v)^2 dx^2 = 2A(u, v) du dv + B(u, v) dx^2. \quad (3.19)$$

In this Kruskal geometry, $uv = 0$ is defined as the horizon, singularity is at $uv = 1$ and both left/right boundaries are located at $uv = -1$. This unperturbed background will obey Einstein's equation which is of the form,

$$E_{\mu\nu} = \kappa T_{\mu\nu}. \quad (3.20)$$

Here, $E_{\mu\nu}$ is the Einstein tensor, $\kappa = 8\pi G_N$ is a constant related to the Newton's constant G_N and $T_{\mu\nu}$ is the stress-energy tensor which is of the form,

$$T_0^{\text{matter}} = 2T_{uv} du dv + T_{uu} du^2 + T_{vv} dv^2 + T_{xx} dx^2. \quad (3.21)$$

It is worth mentioning that this stress tensor accounts for the cosmological constant and is consistent with the Ricci tensor of the unperturbed background. For the unperturbed Einstein equation, solving T_{uu} , T_{vv} and T_{uv} , we get,

$$T_{uu} = \frac{1}{4A(u, v)B(u, v)^2} \left[A(u, v) \partial_u B(u, v)^2 + 2B(u, v) (\partial_u A(u, v) \partial_u B(u, v) - A(u, v) \partial_u^2 B(u, v)) \right], \quad (3.22a)$$

$$T_{uv} = \frac{1}{4B(u, v)^2} \left[2B(u, v) \partial_u \partial_v B(u, v) - \partial_v B(u, v) \partial_u B(u, v) \right], \quad (3.22b)$$

$$T_{vv} = \frac{1}{4A(u, v)B(u, v)^2} \left[A(u, v) \partial_v B(u, v)^2 + 2B(u, v) (\partial_v A(u, v) \partial_v B(u, v) - A(u, v) \partial_v^2 B(u, v)) \right]. \quad (3.22c)$$

3.2.2 Gravitational backreaction due to shock wave

In the previous subsection, we constructed a two-sided Lifshitz black hole geometry in a $(2+1)$ -dimensional background. This section aims to study the back-reacted metric due to a null pulse of energy localized along the $v = 0$ horizon. In the bulk-boundary picture, this means we have inserted an operator in the boundary thermal state at some past time t and let it evolve. Inserting an operator in the boundary leads to releasing a perturbation close to the boundary, which falls into the bulk. From the point of view of the $t = 0$ slice, the energy of this perturbation is exponentially increasing with time t [26]. Thus, we can approximate this perturbation as a null pulse of energy E localized at the $v = 0$ horizon

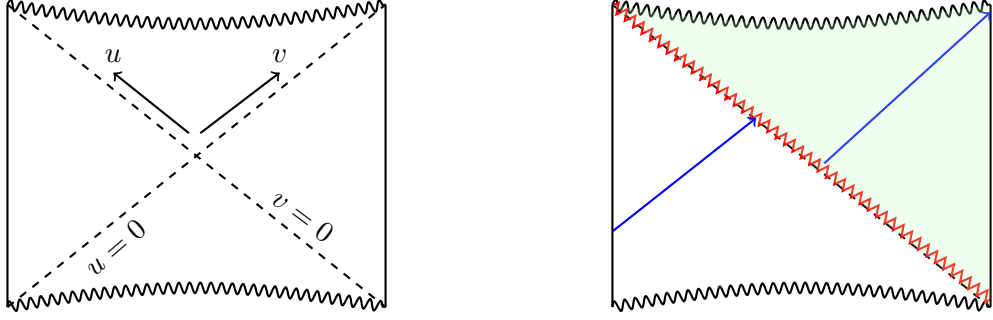


Figure 2. *Left:* Penrose diagram of two-sided geometry. *Right:* A shock wave (red zigzag line) localised along $v = 0$ causes a discontinuity of the $u = 0$ horizon (the blue arrow)

along the u -direction. We must consider the back-reaction of this null pulse in the two-sided geometry.

We consider the following form of the stress-tensor localised at $v = 0$,

$$T_{vv}^{\text{shock}} = E \exp\left(\frac{2\pi t}{\beta}\right) \delta(v) \delta(x). \quad (3.23)$$

The shock wave localised at $v = 0$ horizon is indeed splitting the causal past (white) and future (green) of v . The metric in the green region will change while in the white region, it will remain the same. In the Penrose diagram, we can clearly see the shift along the v -direction. We can write the form of the shift in the following way:

$$\bar{u} = u + \Theta(v) \eta(u, v, x) \rightarrow du = d\bar{u} - \eta(u, v, x) \delta(v) dv, \quad (3.24)$$

$$\bar{v} = v, \quad \bar{x} = x. \quad (3.25)$$

Our goal is to calculate the form of the function $\eta(u, v, x)$ – the shockwave profile. Note that the Heaviside step function $\Theta(v)$ is present to ensure that only the causal future of the pulse is affected by its presence. In terms of these new coordinates $(\bar{u}, \bar{v}, \bar{x})$, we can write the metric as,

$$ds^2 = 2A(\bar{u}, \bar{v}) d\bar{u} d\bar{v} + B(\bar{u}, \bar{v}) d\bar{x}^2 - 2A(\bar{u}, \bar{v}) \eta(u, v, x) \delta(\bar{v}) d\bar{v}^2. \quad (3.26)$$

With this back-reacted form of the metric, we need to calculate a form of $\eta(u, v, x)$ which will obey eq.(3.20). In the above metric,

$$A(\bar{u}, \bar{v}) = \frac{2r(\bar{u}, \bar{v})^{2\xi}}{\alpha^2 \bar{u} \bar{v}} f(r(\bar{u}, \bar{v})), \quad B(\bar{u}, \bar{v}) = r(\bar{u}, \bar{v})^2, \quad (3.27)$$

where we have expressed the radial coordinate r in terms of (u, v) . Now, for the perturbed background, we wish to calculate the stress tensor. The stress tensor for the matter part reads as

$$T_{\mu\nu}^{\text{matter}} = 2[T_{\bar{u}\bar{v}} - 2T_{\bar{u}\bar{u}}\eta(\bar{u}, \bar{v}, x)\delta(\bar{v})] d\bar{u} d\bar{v} + [T_{\bar{v}\bar{v}} + T_{\bar{u}\bar{u}}\eta(\bar{u}, \bar{v}, x)^2\delta(\bar{v})^2 - 2T_{\bar{u}\bar{v}}\eta(\bar{u}, \bar{v}, x)\delta(\bar{v})] d\bar{v}^2 + T_{\bar{u}\bar{u}} d\bar{u}^2 + T_{\bar{x}\bar{x}} d\bar{x}^2. \quad (3.28)$$

We will drop the bar convention for further analyses so that the result looks simpler. Now, we will solve the back-reacted Einstein's equation which is of the form :

$$E_{\mu\nu} = \kappa (T_{\mu\nu}^{\text{matter}} + T_{\mu\nu}^{\text{shock}}) . \quad (3.29)$$

The expressions of $T_{\mu\nu}^{\text{matter}}$ and $T_{\mu\nu}^{\text{shock}}$ is given by (3.28) and (3.23) respectively. Solving the vv component of the perturbed Einstein equation, we get,

$$\begin{aligned} \left[\partial_x^2 - \frac{1}{A(u,v)} \partial_u \partial_v B(u,v) \right] \eta(u,v,x) - \frac{8\pi G_N E B(u,v)}{A(u,v)} e^{2\pi t/\beta} \delta(v) \delta(x) = 0, \\ \Rightarrow [\partial_x^2 - \mathcal{M}(u,v)^2] \eta(u,v,x) = e^{\frac{2\pi}{\beta}(t-t_*)} \delta(v) \delta(x). \end{aligned} \quad (3.30)$$

Where,

$$\mathcal{M}(u,v) = \sqrt{\frac{\partial_u \partial_v B(u,v)}{A(u,v)}}, \quad t_*(u,v) = \frac{\beta}{2\pi} \log \left(\frac{A(u,v)}{8\pi G_N E B(u,v)} \right). \quad (3.31)$$

The function $t_*(u,v)$ has some physical meaning, which we will discuss in the upcoming part. After implementing the values of $A(u,v)$ and $B(u,v)$ to $t_*(u,v)$, it will take a constant form. We can see that the shockwave profile $\eta(u,v,x)$ is obeying an ODE which we can solve easily. In writing the above equation, we assume, $T_{uu} = 0$ near the $v = 0$ horizon [25]. Our task is to solve the equation (3.30) near the horizon. Near the horizon ($v = 0$ or $r = r_h$),

$$A(u,v)|_{v=0} = \frac{8}{1+\xi}, \quad \partial_u \partial_v B(u,v)|_{v=0} = 4r_h^2. \quad (3.32)$$

In taking the derivative of $B(u,v)$ with u and v , we have used the relation (3.18) and performed a chain rule differentiation with r_* . Now, implementing the above two expressions into (3.31), we get,

$$\mathcal{M}(u,v)|_{v=0} = \sqrt{\frac{1+\xi}{2}}, \quad t_* = \frac{\beta}{2\pi} \log \left(\frac{1}{\pi G_N E (1+\xi)} \right), \quad (3.33)$$

where we have considered $r_h = 1$. The constant t_* is called the scrambling time, which is dependent on the anisotropy index ξ . Near the horizon, the equation (3.30) becomes,

$$\left[\partial_x^2 - \frac{1+\xi}{2} \right] \eta(x) = e^{\frac{2\pi}{\beta}(t-t_*)} \delta(x). \quad (3.34)$$

To solve this, first, we will solve the homogeneous equation and get,

$$\eta(x) = \begin{cases} c_1 e^{\mathcal{M}x} + c_2 e^{-\mathcal{M}x} & \text{for } x > 0, \\ c_3 e^{\mathcal{M}x} + c_4 e^{-\mathcal{M}x} & \text{for } x < 0. \end{cases} \quad (3.35)$$

Now, to solve the non-homogeneous equation, we will check the discontinuity of the first derivative of the solution and get,

$$\eta'(\epsilon) - \eta'(-\epsilon) = e^{\frac{2\pi}{\beta}(t-t_*)}, \quad (3.36)$$

where, ϵ is a small parameter $\epsilon \rightarrow 0$. Imposing the continuity of the solution at $x = 0$ and with the discontinuity equation (3.36), we get a relation between the coefficients as,

$$c_1 - c_3 = c_4 - c_2 = \frac{e^{\frac{2\pi}{\beta}(t-t_*)}}{\sqrt{2(1+\xi)}}. \quad (3.37)$$

We will choose $c_2 = c_3 = 0$ and the final solution for the shock will be,

$$\eta(t, x) = \frac{1}{\sqrt{2(1+\xi)}} e^{\frac{2\pi}{\beta}(t-t_*) - \frac{\beta\mathcal{M}}{2\pi}x}. \quad (3.38)$$

This shockwave profile will completely determine the four-point out-of-time ordered function - OTOC. We can identify the commutator $C(t, x)$ in equation (1.3) with the shockwave profile $\eta(t, x)$ and write,

$$\lambda_L = 2\pi T, \quad v_B = \sqrt{\frac{1+\xi}{2}}. \quad (3.39)$$

This Lyapunov exponent agrees with our results of the entanglement wedge method. For the butterfly velocity, this result is found to be the same as obtained from the entanglement wedge result for $d = 2$ in (3.10). Thus, we can claim that these two methods are congruent for a reliable study of chaos in Lifshitz background.

3.3 Pole-skipping

In this subsection, we wish to study the retarded energy density correlation function $G_{T_{00}T_{00}}^R(\omega, k)$ near the pole-skipping point (1.5). This correlation function can be calculated by perturbing the gravitational background (2.2) and imposing ingoing boundary conditions at the black hole horizon. To perform the pole-skipping analysis, it is customary to work with Eddington-Finkelstein coordinates, defined by

$$v = t + r_*, \quad \frac{dr_*}{dr} = \frac{1}{r^{1+\xi}f(r)}, \quad (3.40)$$

where v is the null coordinate and r_* is the tortoise coordinate. With the above coordinate system, the background metric (2.2) is transformed into

$$ds^2 = -r^{2\xi}f(r)dv^2 + 2r^{\xi-1}dvdr + r^2dx^2. \quad (3.41)$$

For our current analysis, we choose the gravity background as the (2+1)-D Lifshitz black hole. Now, to calculate the energy density correlation function, we must perturb the background metric - specifically the sound modes (longitudinal modes). We perturb the background metric as,

$$g_{\mu\nu} \rightarrow g_{\mu\nu} + \delta g_{\mu\nu}(r)e^{-i\omega v + ikx}. \quad (3.42)$$

Here we perform a Fourier transformation to the perturbed mode and choose the wavenumber k along the x -direction. Then, the sound modes will be-

$$\delta g_{vv}, \delta g_{vx}, \delta g_{vr}, \delta g_{rr}, \delta g_{rx}, \delta g_{xx}. \quad (3.43)$$

As the wave points along the x - direction, sound modes are the modes that are only along the (v, r, x) directions. But, imposing radial gauge condition $\delta g_{r\mu} = 0$ and traceless ness condition $g^{\mu\nu}\delta g_{\mu\nu} = 0$, we get some redundant modes and left with–

$$\delta g_{vv}, \delta g_{vx}. \quad (3.44)$$

The retarded energy density Green’s function is governed by the perturbed equations that are regular at the horizon in ingoing EF coordinates. So, we Taylor expand the modes near the horizon as,

$$\delta g_{\mu\nu}(r) = \delta g_{\mu\nu}^{(0)} + (r - r_h)\delta g_{\mu\nu}^{(1)} + \dots, \quad (3.45)$$

Perturbing the sound modes of the background and imposing the regularity condition (3.45) near the black hole horizon, we can achieve the expanded form of Einstein’s equations near the horizon. Our goal is to check whether we get the results of chaos obtained in the previous subsections. For field δg_{vv} , the associated equation of motion is $\delta E_{vv} = \delta T_{vv}$. But, the perturbation to stress tensor δT_{vv} does not vanish necessarily, while δT_v^r vanishes at the horizon [37, 69]. Keeping this in mind, we will set $\delta T_v^r = 0$ to calculate the pole-skipping point connected to chaos. Expanding this equation near the black hole horizon, we get,

$$k \left[2\omega - ir_h^\xi(1 + \xi) \right] \delta g_{vx}^{(0)} + \left[k^2 - ir_h^{2-\xi}\omega + (r_h^2 - r_h^{1+\xi})(1 + \xi) \right] \delta g_{vv}^{(0)} = 0. \quad (3.46)$$

This equation is a constraint relation that gives a relation between the near-horizon coefficients. The above equation is very special at some specific value of frequency(ω) and momentum (k). We can verify that, at $\omega = \omega_* = \frac{i}{2}r_h^\xi(1 + \xi)$, coefficient of $\delta g_{vx}^{(0)}$ is 0. So, at this specific value of ω , we get a relation,

$$\left[k^2 + \frac{1}{2} \left(3r_h - 2r_h^\xi \right) (1 + \xi) \right] \delta g_{vv}^{(0)} = 0. \quad (3.47)$$

For general k , this equation gives rise to $\delta g_{vv}^{(0)} = 0$. However, at $k = k_*$, this equation is automatically satisfied. That means at this specific value ω and k , the δT_v^r is automatically zero and hence they will not impose any constraint on the near-horizon coefficients $\delta g_{vv}^{(0)}$ and $\delta g_{vx}^{(0)}$. This specific value of frequency (ω_*) and momentum (k_*) is called the pole-skipping point. The pole-skipping point we get,

$$\omega_* = \frac{i}{2}r_h^\xi(1 + \xi), \quad k_*^2 = -\frac{1}{2}(3r_h - 2r_h^\xi)(1 + \xi). \quad (3.48)$$

Writing r_h in terms of temperature as $r_h = \left(\frac{4\pi T}{1+\xi} \right)^{1/\xi}$, we can express ω and k in terms of the temperature of the black hole. Now, we can calculate the Lyapunov exponent and butterfly velocity from (1.5) as,

$$\lambda_L = 2\pi T, \quad v_B = \sqrt{\frac{1 + \xi}{2}}. \quad (3.49)$$

Note that, the butterfly velocity (v_B) is a positive real quantity. So, we will take the absolute value of momentum while calculating v_B , i.e. $v_B = \frac{|\omega_*|}{|k_*|}$. From the above expression, we can see that both the Lyapunov exponent and butterfly velocity take the same form as we achieved in our previous subsections. So, we can say that all three methods to compute the chaotic features are reliable. These methods are giving consistent results in higher orders too. One can check it explicitly.

4 Analysis of classical chaos

Here we elucidate a parallel survey of some of the chaos properties, to be precise, eikonal phase shift and Lyapunov exponent, at the classical level. The anatomy of the null geodesics for our specified background and the corresponding turning points adequately serve our purpose. We present a notion of emergent dependency of classical chaos in our framework on the values of these turning points.

4.1 Null geodesic

To carry out the eikonal phase shift in the bulk following, here we will first enunciate the details of the null geodesic for our chosen background. The bulk phase shift for a particle described by a plane wave is given by [91, 92]

$$\delta \equiv -p \cdot (\Delta x), \quad (4.1)$$

where, p denotes the components of the conserved momentum vector and Δx gives the deflections in the corresponding bulk directions. For our metric in equation (2.2) in 2+1 dimension, the conserved energy and momentum are given by

$$p_t = \frac{1}{z^{2\xi}} f(z) \frac{\partial t}{\partial s}, \quad p_x = \frac{1}{z^2} \frac{\partial x}{\partial s}, \quad (4.2)$$

s being the intrinsic affine parameter. These conserved quantities correspond to the two killing vectors ∂_t and ∂_x of our chosen metric during a heavy-heavy-light-light 2-particle scattering, it is convenient to consider that the highly boosted particle consists of large values of conserved momenta. We introduce a parameter $\gamma = \frac{p_x}{p_t}$ which often serves as the impact parameter of the corresponding scattering process. The null geodesic equation is given by

$$g_{\mu\nu} \dot{x}^\mu \dot{x}^\nu = 0, \quad (4.3)$$

which yields

$$\dot{z}^2 = (p_t)^2 z^{2\xi+2} - (p_x)^2 z^4 f(z). \quad (4.4)$$

At the turning point $z = z_0$, z attains extreme value for which we can set $\dot{z}|_{z=z_0} = 0$. Hence, the values of turning points z_0 should satisfy the relation

$$z_0^{2\xi-2} + \frac{\gamma^2}{z_h^{\xi+1}} z_0^{\xi+1} - \gamma^2 = 0. \quad (4.5)$$

The above equation is a polynomial of either integer order or fractional order, depending on the values of the critical exponent ξ . Thus the roots of this equation which are valid for our approach are all real and lie within the singularity and the boundary of the bulk geometry. However, these values of the possible turning points depend on the ratio γ . At this stage, some further crucial remarks on the turning point follow immediately:

- Let us take the assumption that the energy p_t is much greater than the momentum p_x , i.e., $\gamma \gg 1$. With this assumption, taking $z_0 = 1$ equation (4.5) gives,

$$\gamma = \sqrt{\frac{z_h^{\xi+1}}{z_h^{\xi+1} - 1}}. \quad (4.6)$$

It is obvious from the above expression that for any arbitrary value of z_h in between $z_h \rightarrow 0$ and $z_h \rightarrow \infty$, the condition $\gamma \gg 1$ is not satisfied.

- If $\gamma = 1$, i.e., $p_x = p_t$, then the equation (4.5) is not satisfied with $z_0 = 1$.
- Again, for $z_h = 1$, $z_0 = 1$ is not a solution of the null geodesic equation for any arbitrary value of γ .
- The condition (4.6) clearly tells us that, for $z_0 = 1$ as a solution, p_x cannot be less than p_t . Hence, with $p_x < p_t$, we must have $z_0 \neq 1$.
- For any arbitrary value of p_x and p_t ; $z_0 = 0$ does not satisfy the geodesic equation.

From the above conditions, it is evident that $z_0 = 1$, i.e., the horizon for our case and $z_0 = 0$, i.e., the boundary are not good choices of z_0 to carry out our desired study.

4.2 Eikonal phase shift

With the above analysis, here we will exhibit an explicit computation of eikonal phase shift at the turning points z_0 as a nontrivial function of z_0 and ξ . With p_t and p_x as the conserved energy and momentum for our system, the expression of the bulk phase shift takes the form as

$$\delta \equiv p_t(\Delta t) - p_x(\Delta x). \quad (4.7)$$

The deflections along the time and space directions can be found respectively from the expressions of p_t and p_x in (4.2) and the null geodesic equation (4.4) as

$$\Delta t = 2 \int_0^{z_0} \frac{z^{2\xi-1} dz}{f(z) \sqrt{z^{2\xi} - \gamma^2 z^2 f(z)}} = 2a^{\frac{3}{2}} \int_0^{z_0} \frac{z^{2\xi-1} dz}{(a - z^{\xi+1}) \sqrt{(az^{2\xi} - a\gamma^2 z^2 + \gamma^2 z^{\xi+3})}}, \quad (4.8)$$

and

$$\Delta x = 2 \int_0^{z_0} \frac{\gamma z dz}{\sqrt{z^{2\xi} - \gamma^2 z^2 f(z)}} = 2a^{\frac{1}{2}} \gamma \int_0^{z_0} \frac{z dz}{\sqrt{(az^{2\xi} - a\gamma^2 z^2 + \gamma^2 z^{\xi+3})}}, \quad (4.9)$$

where, $a = z_h^{\xi+1}$. Because of the intricate structure of the above integrands, we assume two limiting cases to derive it. Firstly we take the near-boundary zone where $z \leq z_h$. Substituting (4.8) and (4.9) in the expression of the eikonal shift and simplifying, we get for the near boundary zone,

$$\delta \sim \int_0^{z_0} \sqrt{z^{2\xi-2} - \gamma^2(1-\epsilon)} dz \approx p_t \int_0^{z_0} \sqrt{z^{2\xi-2} - \gamma^2} dz, \quad (4.10)$$

where, $\left(\frac{z}{z_h}\right)^{\xi+1} = \epsilon \ll 1$ for $\xi \geq 1$. Now defining a new integration variable $y = \frac{z}{z_0}$ the bulk phase shift is given by

$$\delta \sim \int_0^1 z_0 \sqrt{z_0^{2\xi-2} y^{2\xi-2} - \gamma^2} dy \approx i\gamma z_0 {}_2F_1 \left(-\frac{1}{2}, \frac{1}{2\xi-2}; \frac{2\xi-1}{2\xi-2}; \frac{z_0^{2\xi-2}}{\gamma^2} \right). \quad (4.11)$$

On the other hand, we take the near horizon regime where $z \approx z_h$. In this regime, we can take two limiting cases for the impact parameter γ . When the energy p_t is much greater than the momentum p_x , i.e., $\gamma < 1$, the eikonal phase shift in near horizon case gives

$$\delta = \frac{z_0^\xi}{\xi(\xi+1)} {}_2F_1\left(1, \xi; \xi+1; \frac{z_0}{z_h}\right) = \frac{z_0^\xi}{\xi(\xi+1)} {}_2F_1(1, \xi; \xi+1; z_0). \quad (4.12)$$

Again for the small energy limit, i.e., $p_x \geq p_t$, the impact parameter $\gamma \geq 1$. This, in the near horizon zone, produces,

$$\delta = -\frac{4\gamma(\sqrt{z_0 - z_h} - \sqrt{-z_h})\sqrt{z_h}p_t}{\sqrt{\xi+1}} = -\frac{4\gamma(\sqrt{z_0 - 1} - i)p_t}{\sqrt{\xi+1}}. \quad (4.13)$$

We have assumed $z_h = 1$ in the above expression. It is well-known in the backdrop of gravitational scattering that the real and imaginary nature of the eikonal phase shift respectively represent elastic and inelastic scattering. Thus our study of the classical eikonal phase clearly reveals that the nature of the gravitational scattering between the heavy-heavy-light-light particle collision in the Lifshitz black hole depends on the different regimes taken for the radial coordinate z along with the choices of the impact parameter. For the near boundary case and the large impact parameter limit in the near horizon zone, the imaginary eikonal phase shift implies completely inelastic collisions whereas the small impact parameter limit in the near horizon zone gives real values of δ that stand for elastic scattering. Nevertheless, all the δ 's derived in these limits inevitably happen to be nontrivial functions of the anisotropy index ξ . This allows one to speculate about the dependencies of absorption cross-sections of the above scatterings on the finite anisotropy present in the black hole background.

Again, we use a WKB approximation to verify the consistency of the eikonal phase. Inserting the expressions of time and space deflections in (4.7), we can write,

$$\delta = 2p_t \int_0^{z_0} \frac{\sqrt{z^{2\xi} - \gamma^2 z^2 f(z)}}{z f(z)} dz. \quad (4.14)$$

One may check the emergence of the above eikonal phase via WKB approximation of the solution of the equation of motion of a scalar field. To do this, consider a heavy scalar field ϕ propagating in the chosen Lifshitz background. In the background (2.2), the Klein-Gordon equation of the scalar can be written as

$$z^2 f(z) \partial_z^2 \phi + z^2 \partial_x^2 \phi + z^2 f'(z) \partial_x^2 \phi - \frac{z^{2\xi}}{f(z)} \partial_t^2 \phi - z^\xi f(z) \partial_z \phi + m^2 z^{2+\xi} \phi = 0. \quad (4.15)$$

Performing a Fourier transformation as

$$\phi = \tilde{\phi}(z) e^{i(-p_t t + p_x x)},$$

and taking an ansatz,

$$\tilde{\phi}(z) = e^{ip_t \chi(z)}, \quad (4.16)$$

we can solve for $\chi(z)$. With the large energy ($p_t \gg 1$) limit, the EOM boils down to,

$$(\partial_z \chi(z))^2 = \frac{z^{2\xi} - \gamma^2 z^2 f(z)}{z^2 f^2(z)}. \quad (4.17)$$

Now, taking the positive term of $\partial_z \chi(z)$, we perform an integration and get a solution of $\chi(z)$ as

$$\chi(z) = \int_0^{z_0} \frac{\sqrt{z^{2\xi} - \gamma^2 z^2 f(z)}}{z f(z)} dz. \quad (4.18)$$

where the terms of order $\mathcal{O}(p_t^{-1})$ can be ignored at large energy limit. This is indeed the leading term of the solution. We can see that the WKB approximation of the solution gives us the exact eikonal phase we recovered in (4.14) at leading order.

4.3 Lyapunov exponent

The Lyapunov exponent (λ_L) is one of the key measures in understanding chaotic systems in classical phase space. It quantifies the rate at which the nearby trajectories diverge and provides information on the system's sensitivity to initial conditions. A positive Lyapunov exponent signifies a chaotic system. Mathematically,

$$\delta X(t) = \delta X(0) e^{\lambda_L t},$$

where δX represents the separation between two nearby trajectories. In their study [93], the authors established a connection between the Lyapunov exponent and the effective potential in the radial motion for both massive and massless particles. Building on this framework, we aim to calculate the Lyapunov exponent for a 2+1-dimensional planar Lifshitz black hole in this subsection. Recently, [94] conducted a similar analysis in the context of equatorial hyperscaling-violating black holes, treating Lifshitz black holes as a specific case within their study. For a circular geodesic, the Lyapunov exponent in terms of the second derivative of the effective potential V_{eff} for radial motion is given by [93],[94]

$$\lambda_L = \sqrt{-\frac{V''_{eff}}{2\dot{t}^2}}. \quad (4.19)$$

Now, for a massless particle, the geodesic equation is given in equation (4.4) from which we can calculate the effective potential

$$V_{eff}(z) = \dot{z}^2 = (p_t)^2 z^{2\xi+2} - (p_x)^2 z^4 f(z). \quad (4.20)$$

Where t is the coordinate time. At the turning point $z = z_0$, the condition on circular orbit, i.e., $V_{eff}(z_0) = 0$ and $V'_{eff}(z_0) = 0$ yield

$$\frac{p_t^2}{p_x^2} = z_0^{2-2\xi} f_0, \quad (4.21)$$

and

$$z_0 f'_0 = 2(\xi - 1) f_0, \quad (4.22)$$

where $f_0 = f(z_0)$. Upon substituting equations (4.21) and (4.22) in equation (4.20) we get

$$V''_{eff}(z_0) = -z_0^2 p_x^2 (z_0^2 f_0'' - 2f_0 (2\xi^2 - 5\xi + 3)) . \quad (4.23)$$

Now, utilizing equations (4.2) and (4.23) within equation (4.19), we derive the Lyapunov exponent for the null circular geodesic

$$\lambda_L = \sqrt{\frac{f_0 (z_0^2 f_0'' - 2f_0 (2\xi^2 - 5\xi + 3))}{2z_0^{2\xi}}} . \quad (4.24)$$

Since an unstable circular geodesic meets the condition $V''_{eff} < 0$, it follows from equations (4.23) and (4.24) that λ_L is real whenever the orbit is unstable. It is again straightforward to note that the Lyapunov exponent goes to zero as the turning point z_0 reaches the horizon and becomes infinity when it reaches at boundary $z_0 = 0$, both of which are inconsistent with the expected scenario. Therefore, the above approach of studying the Lyapunov exponent of the theory under consideration does not remain acceptable when the extrema of the null geodesics are chosen in the vicinity of both the boundary and the horizon of the black hole. This also supports our comments in section 4.1 on the possible restrictions on the values $z_0 = 0$ and $z_0 = 1$. At this stage, it is faithful to say that one may carry out a polynomial distribution by using a suitable numerical approach to see what values of z_0 the equation (4.5) can accommodate as its valid solution. We keep this computation for future extensions of our work.

5 Conclusion

We undergo a comparative analysis of three different holography-based approaches to quantum chaos to understand any probable equivalence between them. The asymptotically Lifshitz black hole with arbitrary anisotropy index is chosen to be a fertile gravity background for our work due to its chaotic features which are already explored in various theoretical contexts. The methods involved in this work for studying quantum chaos are entanglement wedge reconstruction, out-of-time-ordered correlators and pole-skipping. All of these approaches are eventually based on the well-known gauge/gravity duality. In the method of entanglement wedge reconstruction, we construct an extremal hypersurface as a constant time slice, famously called Ryu-Takayanagi surface, that extracts out the butterfly velocity at late time. The butterfly velocity occurs to have nontrivial dependence on the anisotropy index of the chosen background. For the unit anisotropy index, it expectantly reduces to that for the planar AdS black hole. For the derivation of OTOCs, we explicitly construct the double-sided Kruskal geometry corresponding to the asymptotically Lifshitz black hole. We introduce a gravitational shockwave backreacting in the Kruskal version of our background. Subsequently, the functional form of the shockwave assumes an exponential form which shows that the system is chaotic and this shockwave profile gives rise to the four-point OTOCs. Such a scenario is somewhat consistent with the previously obtained scenario for a perturbed two-sided AdS black hole. The butterfly velocity and Lyapunov exponent obtained from this shockwave profile are exactly similar to those obtained from

the entanglement wedge method. Finally, in the method of pole-skipping, we again observe the exact same dependency of butterfly velocity as well as the Lyapunov exponent on the anisotropy. As a consequence of the exact matching of the salient chaotic features, we claim that all our chosen methods are equivalent and definitive for the understanding of chaos for the class of asymptotically Lifshitz black holes at the quantum level.

We demonstrate a further investigation of the eikonal phase shift due to heavy-heavy-light-light gravitational scattering and computed the Lyapunov exponent, at the classical level by using the bulk metric both in near-boundary and near-horizon regimes and a detailed study of the associated null geodesics. This reveals that both of these quantities appear to be nontrivial functions of the anisotropy index ξ . We further achieve some obvious restrictions on the possible extrema of the null geodesics where we obtain inconsistent natures of classical eikonal phase shift and Lyapunov exponent. An interesting outcome of the presence of arbitrary anisotropy in our case is that the eikonal phase becomes real or imaginary depending on the near-horizon and near boundary limits of the black hole and the impact parameter. This may allow one to explore the absorption cross-section for both elastic and inelastic scattering in terms of the arbitrary anisotropy index of the asymptotically Lifshitz black hole. We have further verified the eikonal phase by using a WKB approximation of the solution of the Klein-Gordon equation. We understood that in the leading order WKB approximation of the scalar solution, the phase we recovered is the same as that derived from the analysis of the null geodesic equation. It is significant to note that, the eikonal phase approximation from the derivation of the out-of-time-order correlators in (3.38) for near-horizon limit assumes an exponential form similar to $e^{(at-bx)}$ with a ξ -dependent prefactor, a and b being some ξ and β dependent functions. Whereas, for the classical case, it becomes a hypergeometric function of ξ for the near-boundary regime. It would be further interesting to explore the possible connection between these two results which may eventually lead to classical/quantum correspondence in the context of chaos in Lifshitz black hole. Moreover, it would be rather fascinating to extend such a relation between the Lyapunov exponents obtained from quantum and classical analyses. Another intriguing opening is to explicitly evaluate the OTOCs from the systematic construction of the dual thermofield double states of the finite temperature Lifshitz field theory and subsequently study different chaotic features on the field theory side. We hope to come back with some of these ideas in the near future.

Acknowledgments

We would like to thank Debaprasad Maity for his valuable suggestions regarding this work. A special thanks to Diandian Wang and Joydeep Chakravarty for some helpful suggestions in our latest draft. BB is grateful to Arnab Kundu for hosting a visit to SINP, Kolkata, and to Pankaj Chaturvedi for facilitating a visit to NIT, Silchar, where part of this work was conducted. Additionally, BB would like to thank Akhil Sivakumar for various insightful suggestions on this work. AC appreciates Bibhas Ranjan Majhi for hosting a visit to IIT Guwahati, which marked the initiation of this work. AC also acknowledges the financial support from the NSTC, Taiwan (R.O.C.), under grant number 110-2112-M007-015-MY3,

which funded a significant portion of this research. Finally, AC extends sincere thanks to Chong-Sun Chu, Dimitrios Giataganas, Himansu Parihar, and Jaydeep Kumar Basak for their insightful discussions on various aspects of Lifshitz theories, which were extremely beneficial to this work.

References

- [1] J.M. Maldacena, *The Large N limit of superconformal field theories and supergravity*, *Adv. Theor. Math. Phys.* **2** (1998) 231 [[hep-th/9711200](#)].
- [2] O. Aharony, S.S. Gubser, J.M. Maldacena, H. Ooguri and Y. Oz, *Large N field theories, string theory and gravity*, *Phys. Rept.* **323** (2000) 183 [[hep-th/9905111](#)].
- [3] K. Balasubramanian and J. McGreevy, *Gravity duals for nonrelativistic conformal field theories*, *Phys. Rev. Lett.* **101** (2008) 061601.
- [4] W.D. Goldberger, *Ads/cft duality for non-relativistic field theory*, *Journal of High Energy Physics* **2009** (2009) 069.
- [5] J. Maldacena, D. Martelli and Y. Tachikawa, *Comments on string theory backgrounds with non-relativistic conformal symmetry*, *Journal of High Energy Physics* **2008** (2008) 072.
- [6] A. Adams, K. Balasubramanian and J. McGreevy, *Hot spacetimes for cold atoms*, *Journal of High Energy Physics* **2008** (2008) 059.
- [7] S. Kachru, X. Liu and M. Mulligan, *Gravity duals of lifshitz-like fixed points*, *Phys. Rev. D* **78** (2008) 106005.
- [8] V. Keränen, W. Sybesma, P. Szepietowski and L. Thorlacius, *Correlation functions in theories with lifshitz scaling*, *Journal of High Energy Physics* **2017** (2017) .
- [9] M. Kord Zangeneh, B. Wang, A. Sheykhi and Z. Tang, *Charged scalar quasi-normal modes for linearly charged dilaton-lifshitz solutions*, *Physics Letters B* **771** (2017) 257.
- [10] C. Park, *Massive quasinormal mode in the holographic lifshitz theory*, *Phys. Rev. D* **89** (2014) 066003.
- [11] J. Cheyne and D. Mattingly, *Constructing entanglement wedges for Lifshitz spacetimes with Lifshitz gravity*, *Phys. Rev. D* **97** (2018) 066024 [[1707.05913](#)].
- [12] J.K. Basak, A. Chakraborty, C.-S. Chu, D. Giataganas and H. Parihar, *Massless Lifshitz Field Theory for Arbitrary z* , [2312.16284](#).
- [13] X. Bai, B.-H. Lee, T. Moon and J. Chen, *Chaos in Lifshitz Spacetimes*, *J. Korean Phys. Soc.* **68** (2016) 639 [[1406.5816](#)].
- [14] D. Giataganas and K. Sfetsos, *Non-integrability in non-relativistic theories*, *JHEP* **06** (2014) 018 [[1403.2703](#)].
- [15] E. Plamadeala and E. Fradkin, *Scrambling in the quantum lifshitz model*, *Journal of Statistical Mechanics: Theory and Experiment* **2018** (2018) 063102.
- [16] N. Sircar, J. Sonnenschein and W. Tangarife, *Extending the scope of holographic mutual information and chaotic behavior*, *JHEP* **05** (2016) 091 [[1602.07307](#)].
- [17] J.S. Cotler, G. Gur-Ari, M. Hanada, J. Polchinski, P. Saad, S.H. Shenker et al., *Black Holes and Random Matrices*, *JHEP* **05** (2017) 118 [[1611.04650](#)].

- [18] L. Susskind, *Computational Complexity and Black Hole Horizons*, *Fortsch. Phys.* **64** (2016) 24 [[1403.5695](#)].
- [19] A.R. Brown, D.A. Roberts, L. Susskind, B. Swingle and Y. Zhao, *Complexity, action, and black holes*, *Phys. Rev. D* **93** (2016) 086006 [[1512.04993](#)].
- [20] J.M. Magán, *Black holes, complexity and quantum chaos*, *JHEP* **09** (2018) 043 [[1805.05839](#)].
- [21] L. Pausch, E.G. Carnio, A. Rodríguez and A. Buchleitner, *Chaos and ergodicity across the energy spectrum of interacting bosons*, *Physical Review Letters* **126** (2021) .
- [22] P. Kos, B. Bertini and T.c.v. Prosen, *Chaos and ergodicity in extended quantum systems with noisy driving*, *Phys. Rev. Lett.* **126** (2021) 190601.
- [23] X. Dong, D. Wang, W.W. Weng and C.-H. Wu, *A tale of two butterflies: an exact equivalence in higher-derivative gravity*, *JHEP* **10** (2022) 009 [[2203.06189](#)].
- [24] M. Mezei and J. Virrueta, *Exploring the Membrane Theory of Entanglement Dynamics*, *JHEP* **02** (2020) 013 [[1912.11024](#)].
- [25] W. Fischler, V. Jahnke and J.F. Pedraza, *Chaos and entanglement spreading in a non-commutative gauge theory*, *JHEP* **11** (2018) 072 [[1808.10050](#)].
- [26] S.H. Shenker and D. Stanford, *Black holes and the butterfly effect*, *JHEP* **03** (2014) 067 [[1306.0622](#)].
- [27] J. Maldacena, S.H. Shenker and D. Stanford, *A bound on chaos*, *JHEP* **08** (2016) 106 [[1503.01409](#)].
- [28] S.H. Shenker and D. Stanford, *Multiple Shocks*, *JHEP* **12** (2014) 046 [[1312.3296](#)].
- [29] D.A. Roberts, D. Stanford and L. Susskind, *Localized shocks*, *JHEP* **03** (2015) 051 [[1409.8180](#)].
- [30] S.H. Shenker and D. Stanford, *Stringy effects in scrambling*, *JHEP* **05** (2015) 132 [[1412.6087](#)].
- [31] D.A. Roberts and D. Stanford, *Two-dimensional conformal field theory and the butterfly effect*, *Phys. Rev. Lett.* **115** (2015) 131603 [[1412.5123](#)].
- [32] S. Khetrpal, *Chaos and operator growth in 2d CFT*, *JHEP* **03** (2023) 176 [[2210.15860](#)].
- [33] C.-J. Lin and O.I. Motrunich, *Out-of-time-ordered correlators in a quantum ising chain*, *Physical Review B* **97** (2018) .
- [34] Y. Gu and X.-L. Qi, *Fractional Statistics and the Butterfly Effect*, *JHEP* **08** (2016) 129 [[1602.06543](#)].
- [35] S. Das, B. Ezhuthachan, A. Kundu, S. Porey, B. Roy and K. Sengupta, *Out-of-Time-Order correlators in driven conformal field theories*, *JHEP* **08** (2022) 221 [[2202.12815](#)].
- [36] M. Blake, H. Lee and H. Liu, *A quantum hydrodynamical description for scrambling and many-body chaos*, *JHEP* **10** (2018) 127 [[1801.00010](#)].
- [37] M. Blake, R.A. Davison, S. Grozdanov and H. Liu, *Many-body chaos and energy dynamics in holography*, *JHEP* **10** (2018) 035 [[1809.01169](#)].
- [38] S. Grozdanov, *On the connection between hydrodynamics and quantum chaos in holographic theories with stringy corrections*, *JHEP* **01** (2019) 048 [[1811.09641](#)].

- [39] Y. Ahn, V. Jahnke, H.-S. Jeong and K.-Y. Kim, *Scrambling in Hyperbolic Black Holes: shock waves and pole-skipping*, *JHEP* **10** (2019) 257 [[1907.08030](#)].
- [40] M. Blake and R.A. Davison, *Chaos and pole-skipping in rotating black holes*, *JHEP* **01** (2022) 013 [[2111.11093](#)].
- [41] K. Sil, *Pole skipping and chaos in anisotropic plasma: a holographic study*, *JHEP* **03** (2021) 232 [[2012.07710](#)].
- [42] W. Li, S. Lin and J. Mei, *Thermal diffusion and quantum chaos in neutral magnetized plasma*, *Phys. Rev. D* **100** (2019) 046012 [[1905.07684](#)].
- [43] M.A.G. Amano, M. Blake, C. Cartwright, M. Kaminski and A.P. Thompson, *Chaos and pole-skipping in a simply spinning plasma*, *JHEP* **02** (2023) 253 [[2211.00016](#)].
- [44] N. Abbasi and J. Tabatabaei, *Quantum chaos, pole-skipping and hydrodynamics in a holographic system with chiral anomaly*, *JHEP* **03** (2020) 050 [[1910.13696](#)].
- [45] B. Baishya and K. Nayek, *Probing pole-skipping through scalar Gauss-Bonnet coupling*, *Nucl. Phys. B* **1001** (2024) 116521 [[2301.03984](#)].
- [46] B. Baishya, S. Chakrabarti, D. Maity and K. Nayek, *Pole-skipping and chaos in D3-D7 brane*, [2312.01829](#).
- [47] H. Yuan and X.-H. Ge, *Pole-skipping and hydrodynamic analysis in Lifshitz, AdS₂ and Rindler geometries*, *JHEP* **06** (2021) 165 [[2012.15396](#)].
- [48] X. Dong, D. Harlow and A.C. Wall, *Reconstruction of bulk operators within the entanglement wedge in gauge-gravity duality*, *Phys. Rev. Lett.* **117** (2016) 021601.
- [49] A.C. Wall, *Maximin Surfaces, and the Strong Subadditivity of the Covariant Holographic Entanglement Entropy*, *Class. Quant. Grav.* **31** (2014) 225007 [[1211.3494](#)].
- [50] B. Czech, J.L. Karczmarek, F. Nogueira and M. Van Raamsdonk, *The Gravity Dual of a Density Matrix*, *Class. Quant. Grav.* **29** (2012) 155009 [[1204.1330](#)].
- [51] S. Ryu and T. Takayanagi, *Holographic derivation of entanglement entropy from the anti-de Sitter space/conformal field theory correspondence*, *Phys. Rev. Lett.* **96** (2006) 181602.
- [52] M. Mezei and D. Stanford, *On entanglement spreading in chaotic systems*, *JHEP* **05** (2017) 065 [[1608.05101](#)].
- [53] M. Taylor, *Lifshitz holography*, *Class. Quant. Grav.* **33** (2016) 033001 [[1512.03554](#)].
- [54] Y. Sekino and L. Susskind, *Fast Scramblers*, *JHEP* **10** (2008) 065 [[0808.2096](#)].
- [55] P. Hayden and J. Preskill, *Black holes as mirrors: Quantum information in random subsystems*, *JHEP* **09** (2007) 120 [[0708.4025](#)].
- [56] M. Blake, R.A. Davison and D. Vegh, *Horizon constraints on holographic Green's functions*, *JHEP* **01** (2020) 077 [[1904.12883](#)].
- [57] M. Natsuume and T. Okamura, *Nonuniqueness of Green's functions at special points*, *JHEP* **12** (2019) 139 [[1905.12015](#)].
- [58] S. Grozdanov, K. Schalm and V. Scopelliti, *Black hole scrambling from hydrodynamics*, *Phys. Rev. Lett.* **120** (2018) 231601 [[1710.00921](#)].
- [59] X. Wu, *Higher curvature corrections to pole-skipping*, *JHEP* **12** (2019) 140 [[1909.10223](#)].
- [60] D.M. Ramirez, *Chaos and pole skipping in CFT₂*, *JHEP* **12** (2021) 006 [[2009.00500](#)].

- [61] F.M. Haehl, W. Reeves and M. Rozali, *Reparametrization modes, shadow operators, and quantum chaos in higher-dimensional CFTs*, *JHEP* **11** (2019) 102 [[1909.05847](#)].
- [62] S. Das, B. Ezhuthachan and A. Kundu, *Real time dynamics from low point correlators in 2d BCFT*, *JHEP* **12** (2019) 141 [[1907.08763](#)].
- [63] N. Abbasi and K. Landsteiner, *Pole-skipping as order parameter to probe a quantum critical point*, [2307.16716](#).
- [64] M. Natsuume and T. Okamura, *Pole-skipping with finite-coupling corrections*, *Phys. Rev. D* **100** (2019) 126012 [[1909.09168](#)].
- [65] N. Ceplak and D. Vegh, *Pole-skipping and Rarita-Schwinger fields*, *Phys. Rev. D* **103** (2021) 106009 [[2101.01490](#)].
- [66] K.-Y. Kim, K.-S. Lee and M. Nishida, *Holographic scalar and vector exchange in OTOCs and pole-skipping phenomena*, *JHEP* **04** (2021) 092 [[2011.13716](#)].
- [67] S. Grozdanov, *Bounds on transport from univalence and pole-skipping*, *Phys. Rev. Lett.* **126** (2021) 051601 [[2008.00888](#)].
- [68] H.-S. Jeong, K.-Y. Kim and Y.-W. Sun, *Bound of diffusion constants from pole-skipping points: spontaneous symmetry breaking and magnetic field*, *JHEP* **07** (2021) 105 [[2104.13084](#)].
- [69] D. Wang and Z.-Y. Wang, *Pole Skipping in Holographic Theories with Bosonic Fields*, *Phys. Rev. Lett.* **129** (2022) 231603 [[2208.01047](#)].
- [70] Y.-T. Wang and W.-B. Pan, *Pole-skipping of holographic correlators: aspects of gauge symmetry and generalizations*, *JHEP* **01** (2023) 174 [[2209.04296](#)].
- [71] H. Yuan, X.-H. Ge, K.-Y. Kim, C.-W. Ji and Y. Ahn, *Pole-skipping points in 2D gravity and SYK model*, *JHEP* **08** (2023) 157 [[2303.04801](#)].
- [72] M. Natsuume and T. Okamura, *Pole skipping in a non-black-hole geometry*, *Phys. Rev. D* **108** (2023) 046012 [[2306.03930](#)].
- [73] B. Baishya, S. Chakrabarti and D. Maity, *Effect of scalar condensation on fermionic Pole-Skipping*, [2311.05314](#).
- [74] D.N. Kabat and M. Ortiz, *Eikonal quantum gravity and Planckian scattering*, *Nucl. Phys. B* **388** (1992) 570 [[hep-th/9203082](#)].
- [75] G. D’Appollonio, P. Di Vecchia, R. Russo and G. Veneziano, *High-energy string-brane scattering: Leading eikonal and beyond*, *JHEP* **11** (2010) 100 [[1008.4773](#)].
- [76] N.E.J. Bjerrum-Bohr, J.F. Donoghue, B.R. Holstein, L. Planté and P. Vanhove, *Bending of Light in Quantum Gravity*, *Phys. Rev. Lett.* **114** (2015) 061301 [[1410.7590](#)].
- [77] L. Cornalba, M.S. Costa, J. Penedones and R. Schiappa, *Eikonal Approximation in AdS/CFT: From Shock Waves to Four-Point Functions*, *JHEP* **08** (2007) 019 [[hep-th/0611122](#)].
- [78] L. Cornalba, M.S. Costa, J. Penedones and R. Schiappa, *Eikonal Approximation in AdS/CFT: Conformal Partial Waves and Finite N Four-Point Functions*, *Nucl. Phys. B* **767** (2007) 327 [[hep-th/0611123](#)].
- [79] R.C. Brower, M.J. Strassler and C.-I. Tan, *On the eikonal approximation in AdS space*, *JHEP* **03** (2009) 050 [[0707.2408](#)].

- [80] K. Balasubramanian and J. McGreevy, *An Analytic Lifshitz black hole*, *Phys. Rev. D* **80** (2009) 104039 [[0909.0263](#)].
- [81] M. Taylor, *Lifshitz holography*, *Classical and Quantum Gravity* **33** (2016) 033001.
- [82] U.H. Danielsson and L. Thorlacius, *Black holes in asymptotically Lifshitz spacetime*, *JHEP* **03** (2009) 070 [[0812.5088](#)].
- [83] V. Jahnke, K.-Y. Kim and J. Yoon, *On the Chaos Bound in Rotating Black Holes*, *JHEP* **05** (2019) 037 [[1903.09086](#)].
- [84] M. Mezei and G. Sárosi, *Chaos in the butterfly cone*, *JHEP* **01** (2020) 186 [[1908.03574](#)].
- [85] A.P. Reynolds and S.F. Ross, *Butterflies with rotation and charge*, *Class. Quant. Grav.* **33** (2016) 215008 [[1604.04099](#)].
- [86] R.R. Poojary, *BTZ dynamics and chaos*, *JHEP* **03** (2020) 048 [[1812.10073](#)].
- [87] A. Banerjee, A. Kundu and R.R. Poojary, *Rotating black holes in AdS spacetime, extremality, and chaos*, *Phys. Rev. D* **102** (2020) 106013 [[1912.12996](#)].
- [88] A. Saha and S. Gangopadhyay, *Quantum chaos in the presence of non-conformality*, [2401.05814](#).
- [89] A. Alvarez, E. Ayón-Beato, H.A. González and M. Hassaïne, *Nonlinearly charged Lifshitz black holes for any exponent $z > 1$* , *JHEP* **06** (2014) 041 [[1403.5985](#)].
- [90] K.-X. Zhu, F.-W. Shu and D.-H. Du, *Holographic complexity for nonlinearly charged lifshitz black holes*, *Classical and Quantum Gravity* **37** (2020) 195023.
- [91] M. Kulaxizi, G.S. Ng and A. Parnachev, *Black holes, heavy states, phase shift and anomalous dimensions*, *SciPost Phys.* **6** (2019) 065.
- [92] A. Parnachev and K. Sen, *Notes on AdS-Schwarzschild eikonal phase*, *JHEP* **03** (2021) 289 [[2011.06920](#)].
- [93] V. Cardoso, A.S. Miranda, E. Berti, H. Witek and V.T. Zanchin, *Geodesic stability, Lyapunov exponents and quasinormal modes*, *Phys. Rev. D* **79** (2009) 064016 [[0812.1806](#)].
- [94] A.N. Kumara, S. Punacha and M.S. Ali, *Lyapunov Exponents and Phase Structure of Lifshitz and Holographic Violating Black Holes*, [2401.05181](#).